Facile Hydrothermal Synthesis of EAB-type Zeolite under Static Synthesis Conditions

Takeshi Hagio, Jae-Hyeok Park, Yan Lin, Yanqin Tian, Yun Hang Hu, Xinling Li, Yuki Kamimoto and Ryoichi Ichino*

Dr. T. Hagio, J. H. Park, Dr. Y. Kamimoto, Prof. R. Ichino
[1] Institute of Materials Innovation, Institutes of Innovation for Future Society, Nagoya University, Furo-cho, Chikusa-ku, Nagoya, Aichi 464-8601, Japan
[2] Department of Chemical Systems Engineering, Graduate School of Engineering, Nagoya University, Furo-cho, Chikusa-ku, Nagoya, Aichi 464-8603, Japan
E-mail: hagio@mirai.nagoya-u.ac.jp

Dr. Y. Lin, Y. Tian
[3] School of Environmental Science and Engineering, Shanghai Jiao Tong University, 800 Dongchuan Road, Shanghai 200240, China

Prof. Y. H. Hu
[4] Department of Materials Science and Engineering, Michigan Technological University, Houghton, MI 49931, USA

Dr. X. Li
[5] School of Mechanical Engineering, Shanghai Jiao Tong University, 800 Dongchuan Road, Shanghai 200240, China

Keywords: EAB-type zeolite, hydrothermal synthesis, crystallization, static condition

Abstract

Conventionally, EAB-type zeolites are crystallized by hydrothermal synthesis for many days under agitational synthesis conditions such as rotation or stirring. In the present study, EAB-type zeolite is obtained by hydrothermal synthesis within 12 hours under static synthesis conditions for the first time. The effects of crystallization temperature, aging of the precursor sol, and addition of seed crystals are investigated. The results reveal that EAB-type zeolite can be obtained when using a precursor sol with short aging time followed by hydrothermal synthesis in a very narrow temperature range of 110 °C to 120 °C under static synthesis condition. Addition of seed crystals is found to suppress the formation of SOD-type zeolite; the primary phase at high hydrothermal synthesis temperatures, while it does not increase the crystallization rate of EAB-type zeolite. Furthermore, the crystallization behavior at 120 °C is examined by varying the synthesis time. EAB-type zeolite with invariably twinned plate-like

morphology starts to crystallize between synthesis time of 3 to 6 hours at 120 °C under the static synthesis condition.

1. Introduction

Zeolites are a class of crystalline microporous aluminosilicates constructed from tetrahedrally coordinated silica ($SiO_{4/2}$) and alumina ($AlO_{4/2}^-$) units forming a 3-dimensional network by sharing their cornering oxygen atoms.[1,2] Pores with extremely uniform size and shape along with the high tunability of their 3-dimensional pore systems, morphologies, and particle size have encouraged applications in a variety of fields including catalysts, adsorbents, and ion-exchangers.[2-4] Various researcher have dedicated their efforts to the synthesis of zeolites[1-6]; however, the relationship between synthesis descriptors and the resulting zeolite framework still remains unclear in spite of the long history in zeolite synthesis.[6] Thus, collecting information on the effects of crystallization parameters in zeolite synthesis is important, especially for rarely understood zeolites that lack information on their synthesis.

Among various zeolites, EAB-type zeolite is one of the rarely studied zeolite with a 2-dimensional 8 membered ring pore system.[7] EAB is also known to be the structure type of the natural mineral; bellbergite, which was found in 1990s near the Bellberg volcano in Germany.[8] The structure of EAB-type zeolite is closely related to that of ERI-type zeolite and has been mistakenly identified until the structure was precisely determined.[9] It belongs to the diverse family of zeolites known as the ABC-6 family[10], a family of industrial important for catalysts constructed from the stacking of modular 6-ring layers.[6] The frameworks of all ABC-6 zeolites are built by 3 types of parallel 6-ring layers (denoted as A, B, and C, respectively) stacked along the c-direction in hexagonal unit cells[11]. The stacking sequence of EAB-type zeolite can be expressed as AABCCB while that of ERI-type zeolite is AABAAC.[12] The only difference in the structure of EAB and ERI is the interchange of single and double rings in the structure.[9] Despite the fact that EAB-type zeolite was the first

8 membered ring zeolite synthesized using an organic structure directing agent (OSDA)[1], reports on its synthesis is extremely limited. The first artificial synthesis of EAB-type zeolite (also called TMA-E) was reported by Aiello and Barrer[13] in 1970, before the discovery of bellbergite, by using precursor sol containing a combination of sodium cations and OSDA; tetramethylammonium hydroxide (TMAOH). A pure phase was crystallized by hydrothermal synthesis at 80 °C for 7 days under rotation from a precursor sol with a limited molar composition of $4Na_2O:15SiO_2:1Al_2O_3:8OSDA:400\text{-}480H_2O$ and $2Na_2O:15SiO_2:1Al_2O_3:16OSDA:400\text{-}500H_2O$. In 1981, Meier and Groner[9] challenged to modify the composition of the precursor sol and succeeded in synthesizing EAB-type zeolite by preparing a precursor sol with the composition of $3.51Na_2O:13.60SiO_2:1.00Al_2O_3:167.26OSDA:372H_2O$ followed hydrothermal synthesis at 80 °C for 4 to 5 days under intensive stirring. Afterwards, the synthesis procedure was verified by B. Schoeman and B. Subotic[14] and was found to be reproducible by hydrothermal synthesis at 80 °C for 14 days under rotation from a precursor sol with a molar composition of $3Na_2O:15SiO_2:1Al_2O_3:10OSDA:500H_2O$. While several researchers have reported the synthesis of EAB-type zeolites, conventional synthesis are all carried out under agitational conditions such as rotation or stirring and it requires more than several days to crystallize the EAB-type zeolite.

Meanwhile, agitational synthesis conditions; such as rotation and stirring during the hydrothermal synthesis process, are reported to be important factors affecting the crystallization speed and structure type of the synthesized zeolite. Gürey et al[15] reported that the change in synthesis condition from agitational to static for MWW-type zeolite caused decreased crystallization rate, narrower crystallization conditions, and generation of impurity phase before reaching complete crystallization. Liu et al.[16] also found that only synthesis under rotation resulted in pure YFI-type zeolite while static synthesis led to inclusion of MFI-type zeolite as an impurity phase. Kubota et al.[17] found that crystallization of CFI-type

zeolite was successful under agitational synthesis conditions but not under static ones (resulting in amorphous product) from a same precursor sol when using Teflon-lined containers. Derewinski and Machowska[18] found that agitational synthesis led to crystallization of TON-type zeolite while static synthesis resulted in MEL-type zeolite from the same precursor sol and synthesis temperature and time. A similar shift was observed by Kawase et al.[19] that the structure type changed from MFI-type zeolite to TON-type zeolite when the synthesis was changed from static to agitational conditions. In addition, in the same ABC-6 family with EAB-type zeolite, Ahn et al.[20] reported that AFV-type zeolite crystallized under agitational synthesis while LEV-type zeolite crystallized under static synthesis with using the same precursor sol. From these reports, changing agitational synthesis conditions to static synthesis conditions are challenging from the view point of obtaining a pure single phase and increase in crystallization rate. Furthermore, the synthesis of EAB-type zeolite under static conditions in short synthesis time have not been reported yet.

The objective of this study is to confirm the possibility of synthesizing the EAB-type zeolite under a static condition and within a short time. The effect of hydrothermal synthesis temperature, aging time of the precursor sol, and addition of seed crystals were investigated using the precursor sol with a composition verified to be reproducible under agitational conditions.[14] Furthermore, the crystallization behavior was examined by carrying out synthesis at various time intervals using the condition that produced EAB-type zeolite in the former experiment.

2. Results and Discussion

The effect of agitational synthesis conditions on EAB-type zeolite synthesis was considered by comparing the product obtained by a static synthesis using a precursor sol composition of a previous report (See Supporting Information). An amorphous product or EAB-type zeolite including intense hydroxy sodalite as impurity phase were obtained under static condition,

implying the importance of a agitational synthesis condition to obtain pure EAB-type zeolite (**Figure S1**). To explore the possibility of synthesizing EAB-type zeolite under static synthesis conditions and within a short synthesis time, various experimental conditions were tested. The experimental conditions carried out in this study are listed in Table 1.

2.1. Effect of Hydrothermal Synthesis Temperature

Hydrothermal synthesis temperature is one of the most important factors determining the framework type in the zeolite synthesis.[21] **Figure 1** shows the X-ray diffractograms of products hydrothermally synthesized for 12 hours at various temperatures between 80 to 160 °C (Product No. P1 to P8). Only broad peaks were observed below 100 °C, meaning that the product was amorphous and no crystallization took place. Weak peaks from a crystalline substance were recognized when the temperature was increased to 110 °C, though still containing a significant fraction of amorphous phase. The peak position of the detected crystalline substance well corresponded to those of EAB-type zeolite registered in the database provided by the International Zeolite Association[7], evidencing that EAB-type zeolite can be crystallized under the static synthesis condition within 12 hours. This is, to the best of our knowledge, the shortest synthesis time reported for the synthesis of EAB-type zeolite. Although the effect of agitational synthesis conditions on zeolite crystallization is still not clarified, agitational synthesis conditions are considered to maintain the uniformity of composition within the precursor sol.[18] Thus, the increase in synthesis temperature may have enabled nucleation of EAB-type zeolite before inhomogeneity occurred within the sol. The peak intensity drastically increased at 120 °C, implying that the crystallization was enhanced by the increase in synthesis temperature. However, when the hydrothermal synthesis temperature was further increased to 130 °C, new peaks around 24.5 and 34.5 degrees started to appear. Peaks of the new phase was associated with hydroxy sodalite; a 6 membered ring zeolite with the SOD structure. The SOD-type zeolite became dominent at 140 °C and

became the only phase at 160 °C. This indicates that SOD-type zeolite was more stable compared to EAB-type zeolites at elevated temperatures. The adequate hydrothermal synthesis temperature for EAB-type zeolite seemed to be in the narrow range between 110 to 120 °C. **Figure 2** shows the FE-SEM images of products hydrothermally synthesized for 12 hours at various temperatures between 80 to 160 °C (Product No. P1 to P8). Particles with irregular shapes were observed below 100 °C, which were possibly the amorphous aluminosilicates. Meanwhile, crystals with invariably twinned plate-like morphologies were observed in the temperature range of 110 to 120 °C. This morphology well resembled that of EAB-type zeolite synthesized at 80 °C under agitation reported in a previous study[9], implying these invariably twinned plate-like crystals were EAB-type zeolites detected in the X-ray diffractograms. This morphology was preserved to some extent until 140 °C, even though SOD-type zeolite gradually became the dominant phase. Observation at higher magnification showed that surface of the invariably twinned plate-like crystals were comprised of round particles below 120 °C and became more angular above 130 °C. The morphologies of the angular particles are similar to those of SOD-type zeolite reported by Sánchez-Hernández et al.[22] SOD-type zeolite belongs to the same family of zeolites with the EAB-type zeolite called the ABC-6[12] and it is reported that SOD-type zeolite can be obtained by breaking only one twelfth of the original siloxane bridges in the EAB framework.[9] (Similarity in stacking sequence of EAB- and SOD-type zeolite is shown in **Figure S2**) Actually, calcination of EAB-type zeolite above 360 °C was reported to result in phase transition to SOD-type zeolite.[13] The increase in hydrothermal synthesis temperature may have caused distruction of the siloxane bridges or densification of the structure, leading to formation of the SOD-type zeolite in the present study as well.

2.2. Effect of Aging of Precursor sol

Aging of precursors is known as an effective method that can increase the crystallization rate and yields in zeolite synthesis.[23,24] Moreover, the effect of reagents reacting during the preparation step of precursor sol may provide similar conditions to agitational synthesis conditions. Thus, the effect of aging was investigated at fixed hydrothermal synthesis temperature of 110 °C, which yielded EAB-type zeolite with incomplete crystallization. **Figure 3** shows the X-ray diffractograms of products synthesized at 110 °C for 12 hours with short aging time of 40 min and with long aging time of 24 hours (Product No. P4 and P9). The two different aging conditions led to completely different results. A long aging time resulted in crystallization of various zeolite frameworks, including not only EAB, but also SOD, LTA, and FAU. The peak intensity of EAB-type zeolite was not intensified by the aging of the precursor sol, meaning that aging process did not help the crystallization of EAB-type zeolite. **Figure 4** shows the FE-SEM images of products synthesized at 110 °C for 12 hours with short and long aging time of 40 min and 24 hours, respectively (Product No. P4 and P9). Crystals with various morphologies were observed in the condition with aging time of 24 hours. The typical morphologies of the impurity phases were observed, which were cubic for LTA- and octahedral for FAU-type zeolites, respectively, along with the invariably twinned plate-like crystals of EAB-type zeolite. LTA- and FAU-type zeolites are also known to be crystallized from a precursor sol containing sodium and TMA cations.[25] Fan et al.[26] considered the aging effect against competitive crystallization of LTA- and FAU-type zeolites from a precursor sol containing sodium and TMA cations. They speculated that the 4 rings and/or double 4 rings (precursors of LTA) in the precursor sol was converted to 6 rings and/or double 6 rings (precursors of FAU) by the slow reactions with amorphous silica during the aging step. Such precursors of LTA and FAU might have been formed during the aging process in this study due to the compositional similarity of the precursor sol, resulting in the crystallization of various impurity phases in this study. To conclude, a longer aging time

could not replace the agitational conditions during the synthesis stage and a short aging time was found to be adequate in the crystallization of EAB-type zeolite.

2.3. Effect of Seed Crystal Addition

Addition of seed crystals to the precursor sol is another method reported to increase the crystallization rate, and in some cases, direct the desired crystalline phase.[2,23,27] Thus, the effect of seed crystal addition was examined. **Figure 5** shows the X-ray diffractograms of products synthesized in the presence of seed crystal for 12 hours at temperatures between 90 to 130 °C (Product No. P10 to P14) along with their intensity difference; ΔI, compared to those synthesized in the absence of seed crystals. ΔI was calculated according to the following equation (**Equation 1**),

$$\Delta I = \Delta I_{\text{seed}} - \Delta I_0 \qquad (1)$$

Here, ΔI_{seed} and ΔI_0 are the intensities of the X-ray diffractions from the product synthesized in the presence and absence of seed crystals, respectively. Because the peak intensity of EAB-type zeolite did not change regardless of the presence of seed crystals at 110 and 120 °C, which can be confirmed from the constant ΔI value of the products synthesized, it can be said that seed crystals did not work as crystallization promoters of EAB-type zeolite in this study. The weak peaks of EAB-type zeolite detected in the products obtained at 90 and 100 °C must be attributed to the remaining seed crystals, estimated to be approximately 10 mass% of the collected product. Indeed, the X-ray diffractograms obtained from a mixture of EAB-type zeolite synthesized at 120 °C and amorphous aluminosilicate produced by synthesis at 90 °C for 12 hours in the absence of seed crystals in a weight ratio of 1 to 9 showed nearly the same reflection (**Figure S3**). On the other hand, a sharp decrease in the peak intensity of SOD-type zeolite was observed in the synthesis carried out at 130 °C, evidenced by the decrease in ΔI at all 2 theta positions corresponding to SOD-type zeolites. Additions of seed crystals seemed to

suppress the formation of SOD-type zeolite, slightly widening the applicable temperature range for synthesis of EAB-type zeolite. **Figure 6** shows the FE-SEM images of products synthesized in the presence of seed crystal for 12 hours at temperatures between 90 to 130 °C (Product No. P10 to P14). EAB-type zeolite crystals with invariably twinned plate-like morphologies were observed in all products as anticipated from the X-ray diffractograms. The surface of the product synthesized at 130 °C seemed to be only partially changed to angular SOD-type zeolite particles. Observation seemed to support the anticipation that the seed crystals suppresses the formation of SOD-type zeolite.

2.4. Crystallization behavior

Considering the results obtained so far, the crystallization behavior was examined using the condition synthesized at 120 °C in the absence of seeds. **Figure 7** shows the X-ray diffractograms of products synthesized at 120 °C for various time intervals (Product No. P15 to P18). No sign of crystallization was observed within 3 hours of synthesis. When the hydrothermal synthesis time reached 6 hours, weak peaks of EAB-type zeolite were detected. This indicates that crystallization of EAB-type zeolite occurred between 3 to 6 hours of synthesis. After 12 hours of synthesis, EAB-type zeolite with high crystallinity was obtained. This was almost one-tenth of the synthesis time reported in most previous studies on preparation of EAB-type zeolite, indicating the superior crystallization rate in the conditions found in this study. **Figure 8** shows the FE-SEM images of products synthesized at 120 °C for time intervals corresponding to **Figure 7**. Amorphous aluminosilicate particles with irregular shapes, similar to those observed at hydrothermal synthesis at low temperatures, were observed at synthesis times of 1.5 and 3 hours. The EAB-type zeolite crystals with invariably twinned plate-like morphologies were found in small portion after 6 hours of synthesis, which corresponds to the change seen in X-ray diffractograms. The size of the EAB-type zeolite crystals became larger by elongating the synthesis time, implying the crystal

growth continuously proceeded during the synthesis. Agitational synthesis conditions during the hydrothermal synthesis process is reported to be essential in some cases to derive a particular zeolite framework, such as CFI-type zeolite (CIT-5)[17], TON-type zeolite[18,19] and AFV-type zeolite (SAPO-57)[20]; however, the present study revealed that EAB-type zeolite can be crystallize under static synthesis conditions.

3. Conclusion

We have succeeded in crystallizing EAB-type zeolite by hydrothermal synthesis under static synthesis conditions and a short time within 12 hours for the first time. The results reveal that a precursor sol with short aging time followed by hydrothermal synthesis in a very narrow temperature range of 110 to 120 °C was adequate for crystallization of EAB-type zeolite. Long aging time of the precursor sol and high hydrothermal synthesis temperatures was found to have adverse effect on the synthesis of EAB-type zeolites, leading to generation of impurity phases with LTA, FAU and SOD structure. Addition of seed crystals did not increase the crystallization rate of EAB-type zeolite but suppressed the formation of SOD-type zeolite. Furthermore, it was found that crystallization of EAB-type zeolite started to take place between 3 to 6 hours when synthesized at 120 °C under the static synthesis condition, indicating a decrease in synthesis time of almost one order of magnitude compared to previous studies.

4. Experimental Section

Materials: Colloidal silica containing 30 mass% of silica (LUDOX® HS-30, Sigma Aldrich), Aluminum hydroxide ($Al_2O_3 \cdot 4.9H_2O$, Sigma Aldrich), and sodium hydroxide (NaOH, purity ≥97 %, Nacalai Tesque) were used as the silica source, alumina source, and alkali source, respectively. Solution containing 15 mass% tetramethylammonium hydroxide (TMAOH, Wako) was used as the organic structure directing agent (OSDA) for EAB-type zeolite.

Synthesis of EAB-type zeolite: The precursor sol with a molar composition of $3Na_2O:15SiO_2:1Al_2O_3$: 10OSDA:$500H_2O$, as reported in a previous study for agitational conditions[14], was selected to consider the synthesis of the EAB-type zeolite under static conditions. The typical synthesis procedure for EAB-type zeolite synthesis was as follows. Distilled water (3.01 g), NaOH pellets (0.46 g), and 15 mass% TMAOH solution (11.50 g) was first added into a polytetrafluoroethylene container and stirred until the NaOH pellets were completely dissolved (approximately 5 min). To this solution, $Al_2O_3 \cdot 4.9H_2O$ (0.36 g) was added and completely dissolved by stirring (approximately 5 min). Then, colloidal silica (5.67 g) was added dropwise to the mixture and aged under continuous stirring for 40 min or 24 hours at room temperature of approximately 25 °C. After aging, the obtained precursor sol (20.00 g) was transferred to a 25 ml Teflon-lined stainless-steel autoclave reactor and sonicated for 5 min. For conditions using seed crystals, seed crystals were added into the reactor before the precursor sol was transferred into the reactor. The hydrothermal synthesis was conducted under static conditions at various temperatures and time intervals under autogenous pressure using a convection oven (OFW-300S-R, AS ONE Corporation). The heating rate was fixed to 200 °C per hour. The synthesized products were collected and rinsed with ion-exchanged water by centrifugation at 3,000 rpm for 5 iterations, completely dried, and ground using an agate mortar.

Characterization of synthesized products: The crystalline phases of the synthesized products were examined using a X-ray diffractometer (RINT-2500TTR, Rigaku Corporation) using Cu Kα radiation (λ =1.5405 Å) generated at 40 kV and 30 mA. The X-ray diffractograms were collected over the angular range of 2 theta of 5 to 35 degrees with a step interval of 0.02 degrees. The morphologies of the synthesized products were observed using a field emission scanning electron microscope (FE-SEM; JSM-6330F, JEOL).

Supporting Information

Supporting Information is available from the Wiley Online Library or from the author.

Acknowledgements

This work was partially supported by JST SICORP Grant Number JPMJSC18H1, Japan, and Project of Creation of Life Innovation Materials for Interdisciplinary and International Researcher Development of the Ministry of Education, Culture, Sports, Science and Technology, Japan.

Conflict of Interest

The authors declare no conflict of interest.

Received: ((will be filled in by the editorial staff))
Revised: ((will be filled in by the editorial staff))
Published online: ((will be filled in by the editorial staff))

References

[1] M. Dusselier, M. E. Davis, *Chem. Rev.* **2018**, *118*, 5265.

[2] K. Itabashi, Y. Kamimura, K. Iyoki, A. Shimojima, T. Okubo, *J. Am. Chem. Soc.* **2012**, *134*, 11542.

[3] S. Banno, K. Komura, *Cryst. Res. Technol.* **2018**, *53*, 1800036.

[4] C. S. Cundy, P. A. Cox, *Chem. Rev.* **2003**, *103*, 663.

[5] M. D. Oleksiak, J. D. Rimer, *Rev. Chem. Eng.* **2014**, *30*, 1.

[6] K. Muraoka, Y. Sada, D. Miyazaki, W. Chaikittisilp, T. Okubo, *Nat. Commun.* **2019**, *10*, 4459.

[7] C. Baerlocher, L. B. McCusker, Database of Zeolite Structures, http://www.iza-structure.org/databases/, accessed: August, 2020.

[8] B. Rüdinger, E. Tillmanns, G. Hentschel, *Mineral. Petrol.* **1993**, *48*, 147.

[9] W. M. Meier, M. Groner, *J. Solid State Chem.* **1981**, *37*, 204.

[10] E. Kianfar, *Rev. Inorg. Chem.* **2019**, *39*, 157.

[11] Y. Li, X. Li, J. Liu, F. Duan, J. Yu, *Nat. Commun.* **2015**, *6*, 8328.

[12] S. Kulprathipanja, *Zeolites in Industrial Separation and Catalysis*, Wiley-VHC, Hoboken, NJ, USA **2010**.

[13] R. Aiello, R. M. Barrer, *J. Chem. Soc. A* **1970**, 1470.

[14] H. Robson, K. P. Lillerud, *Verified Syntheses of Zeolitic Materials Second Revised Edition*, Elsevier Science, Amsterdam, NLD **2001** Ch. 39.

[15] I. Güray, J. Warzywoda, N. Baç, A. Sacco Jr., *Micropor. Mesopor. Mater.* **1999**, 31, 241.

[16] Q. Liu, Y. Yoshida, N. Nakazawa, S. Inagaki, Y. Kubota, *Materials* **2020**, 13, 2030.

[17] Y. Kubota, S. Tawada, K. Nakagawa, C. Naitoh, N. Sugimoto, Y. Fukushima, T. Hanaoka, Y. Imada, Y. Sugi, *Micropor. Mesopor. Mater.* **2000**, 37, 291.

[18] M. Derewinski, M. Machowska, *Stud. Surf. Sci. Catal.* **2004**, 154, 349.

[19] R. Kawase, A. Iida, Y. Kubota, K. Komura, Y. Sugi, K. Oyama, H. Itoh, *Ind. Eng. Chem. Res.* **2007**, 46, 1091.

[20] N. H. Ahn, S. Seo, S. B. Hong, *Catal. Sci. Technol.* **2016**, *6*, 2725.

[21] W. Kim, D. Choi, S. Kim, *Mater. Trans.* **2010**, *51*, 1694.

[22] R. Sánchez-Hernández, A. López-Delgado, I. Padilla, R. Galindo, S. López-Andrés, *Micropor. Mesopor. Mater.* **2016**, *226*, 267.

[23] F. Schüth, K. S. W. Sing, J. Weitkamp, *Handbook of Porous Solids*, Wiley-VHC, Hoboken, NJ, USA **2002**, Ch. 4.2.2.

[24] D. M. Ginter, A. T. Bell, C. J. Radke, *Zeolites* **1992**, *12*, 742.

[25] S. Yang, Q. Li, M. Wang, A. Navrotsky, *Micropor. Mesopor. Mater.* **2006**, *87*, 261.

[26] W. Fan, S. Shirato, F. Gao, M. Ogura, T. Okubo, *Micropor. Mesopor. Mater.* **2006**, *89*, 227.

[27] Ö. Güvenir, H. Kalıpçılar, A. Çulfaz, *Cryst. Res. Technol.* **2009**, *44*, 293.

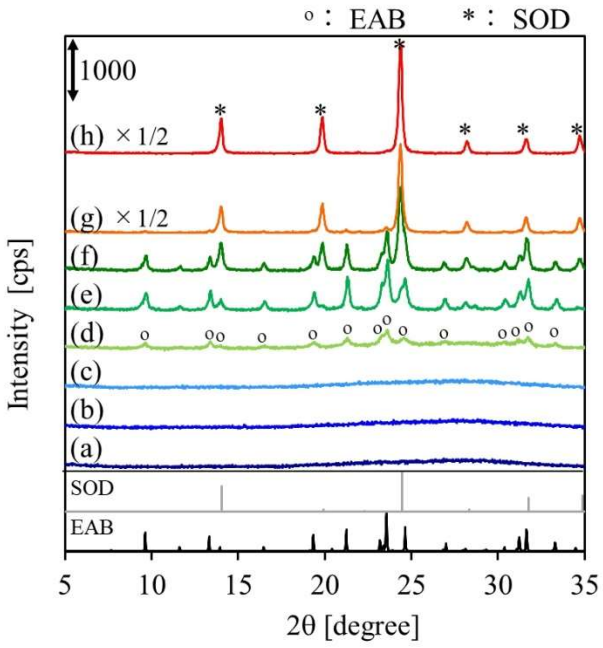

Figure 1. X-ray diffractograms of products synthesized at (a) 80 °C, (b) 90 °C, (c) 100 °C, (d) 110 °C, (e) 120 °C, (f) 130 °C, (g) 140 °C, and (h) 160 °C for 12 hours.

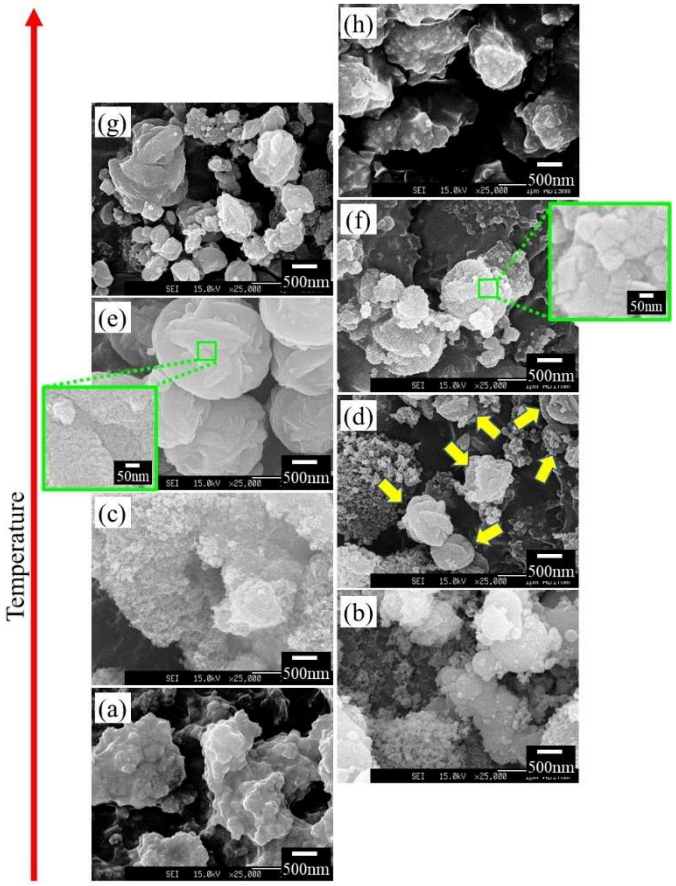

Figure 2. FE-SEM images of products synthesized at (a) 80 °C, (b) 90 °C, (c) 100 °C, (d) 110 °C, (e) 120 °C, (f) 130 °C, (g) 140 °C, and (h) 160 °C for 12 hours.

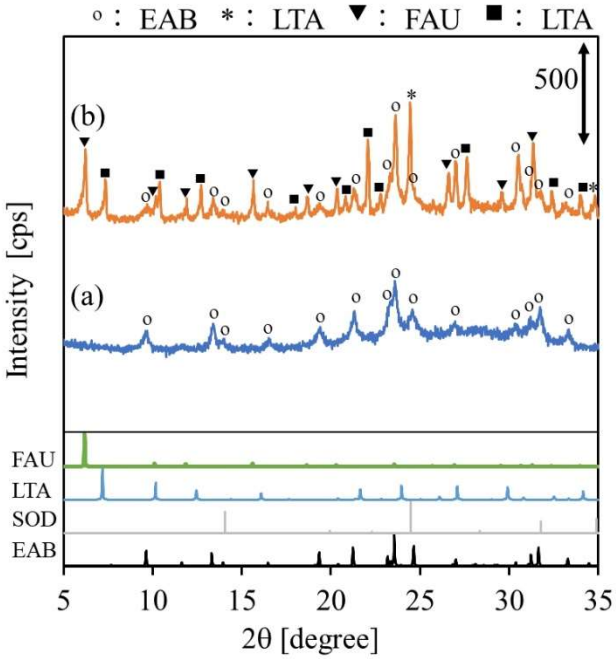

Figure 3. X-ray diffractograms of products synthesized at 110 °C for 12 hours (a) with short aging time of 40 min and (b) with long aging time of 24 hours.

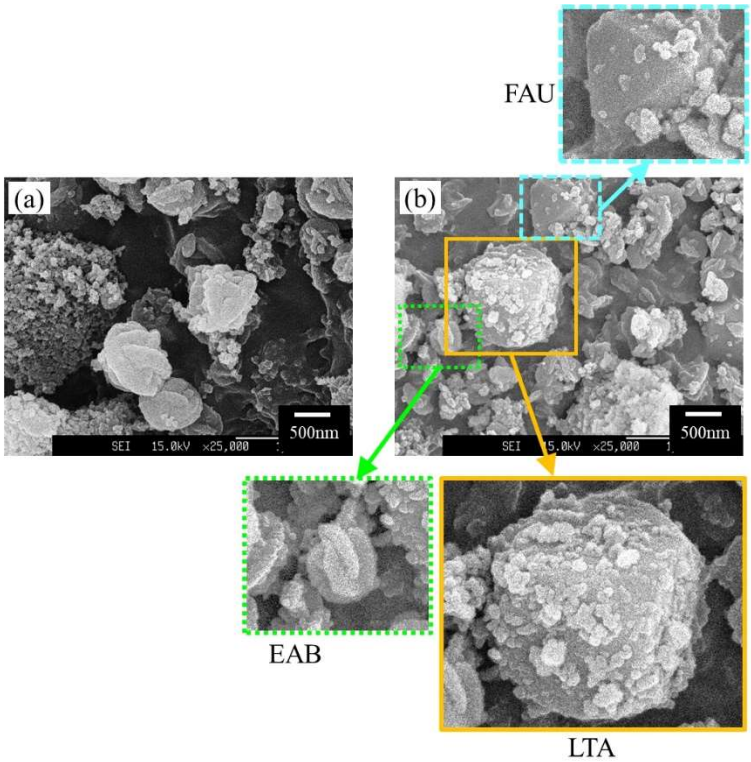

Figure 4. FE-SEM images of products synthesized at 110 °C for 12 hours (a) with short aging time of 40 min and (b) with long aging time of 24 hours.

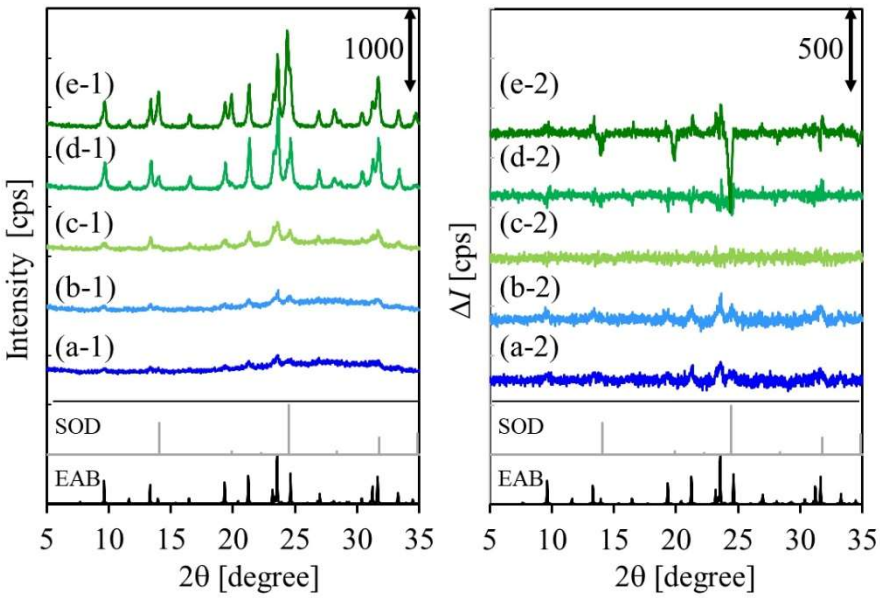

Figure 5. X-ray diffractograms of products synthesized at (a-1) 90 °C, (b-1) 100 °C, (c-1) 110 °C, (d-1) 120 °C, (e-1) 130 °C for 12 hours in the presence of seed crystals and (a-2, b-2, c-2, d-2, e-2) their intensity difference compared to those synthesized without seed crystals.

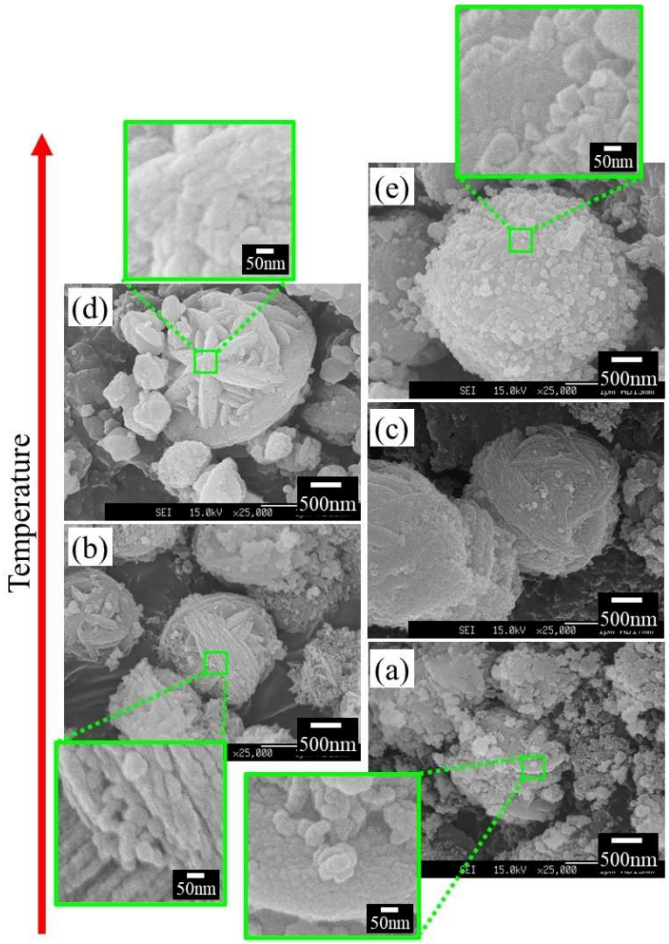

Figure 6. FE-SEM images of products synthesized at (a) 90 °C, (b) 100 °C, (c) 110 °C, (d) 120 °C, (e) 130 °C for 12 hours in the presence of seed crystals.

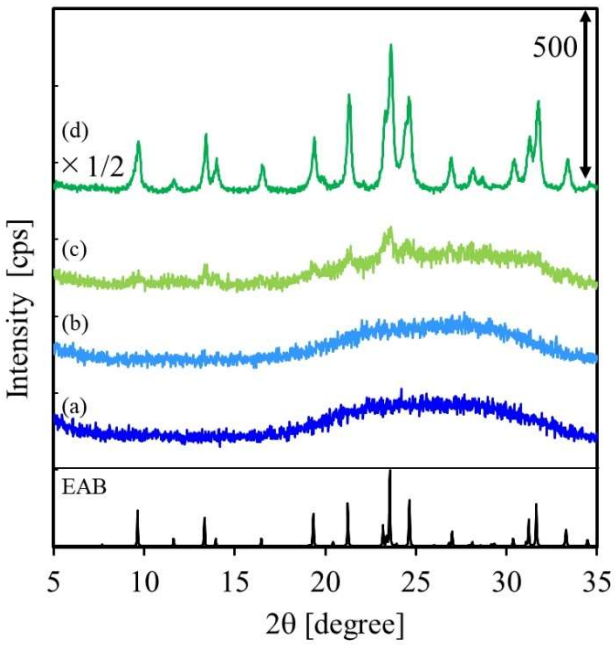

Figure 7. X-ray diffractograms of products synthesized at 120 °C for (a) 1.5 hours (b) 3 hours, (c) 6 hours and (d) 12 hours without seed crystals.

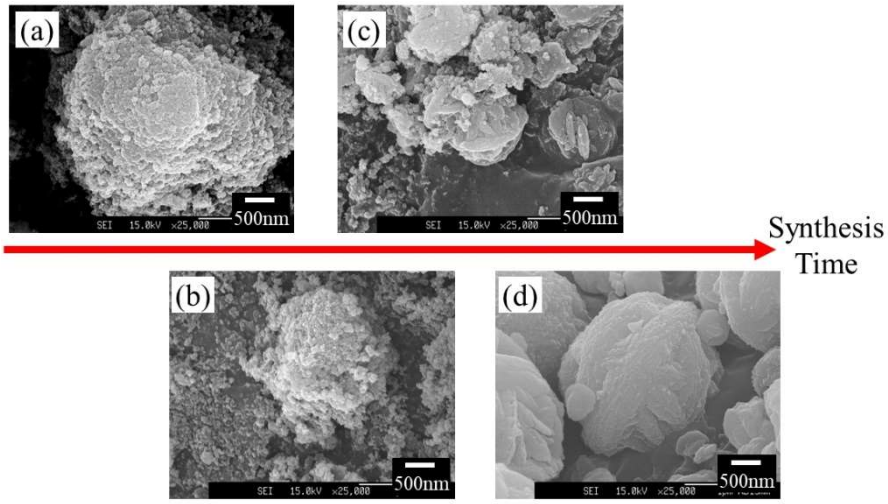

Figure 8. FE-SEM images of products synthesized at 120 °C for (a) 1.5 hours, (b) 3 hours, (c) 6 hours and (d) 12 hours without seed crystals.

Table 1. List of synthesis conditions investigated in this study

Product No.	Precursor sol[a)] aging time	Seed	Hydrothermal condition		Phase
			Temp. [°C]	Time [hours]	
P1	40 min	–	80	12	Am
P2	40 min	–	90	12	Am
P3	40 min	–	100	12	Am
P4	40 min	–	110	12	Am+EAB
P5	40 min	–	120	12	EAB
P6	40 min	–	130	12	EAB+SOD
P7	40 min	–	140	12	SOD(+EAB)
P8	40 min	–	160	12	SOD
P9	24 hours	–	110	12	EAB+LTA+FAU+SOD
P10	40 min	+[b)]	90	12	Am(+EAB)
P11	40 min	+[b)]	100	12	Am(+EAB)
P12	40 min	+[b)]	110	12	Am+EAB
P13	40 min	+[b)]	120	12	EAB
P14	40 min	+[b)]	130	12	EAB(+SOD)
P15	40 min	–	120	1.5	Am
P16	40 min	–	120	3	Am
P17	40 min	–	120	6	Am+EAB
P18	40 min	–	120	12	EAB

[a)] Composition of the precursor sol was fixed to be $3Na_2O:15SiO_2:1Al_2O_3:10OSDA:500H_2O$ (molar ratio), [b)] Product No. 5 was used as seeds, Am: amorphous phase

TABLE OF CONTENTS

- EAB-type zeolite was synthesized under static synthesis conditions, for the first time.
- Narrow hydrothermal synthesis temperature range and short aging time were found to be key factors.
- Addition of seed crystal were found to restricted the formation of impurity phases.
- Crystallization behavior at 120 °C showed EAB-type zeolite could be crystallized within 12 hours, which is the shortest synthesis time reported.